

SAVE THE DATE



01 - 03, December

HNBK International Convention Center

ASGO 2023

TAIPEI www.asgo2023.org



The 8th Biennial Meeting of Asian
Society of Gynecologic Oncology

Original Article



Anti-cancer effect of fenbendazole-incorporated PLGA nanoparticles in ovarian cancer

Chi-Son Chang ^{1,*}, Ji-Yoon Ryu ^{2,*}, June-Kuk Choi ³, Young-Jae Cho ²,
Jung-Joo Choi ², Jae Ryoung Hwang ², Ju-Yeon Choi ², Joseph J. Noh ¹,
Chan Mi Lee ⁴, Ji Eun Won ⁴, Hee Dong Han ⁵, Jeong-Won Lee ^{1,6}

OPEN ACCESS

Received: Oct 6, 2022
Revised: Jan 12, 2023
Accepted: Mar 22, 2023
Published online: Apr 24, 2023

Correspondence to

Jeong-Won Lee





Department of Obstetrics and Gynecology,
Samsung Medical Center, Sungkyunkwan
University School of Medicine, 81 Irwon-ro,
Gangnam-gu, Seoul 06351, Korea.
Email: garden.lee@samsung.com

*Chi-Son Chang and Ji-Yoon Ryu contributed
equally to this paper.

© 2023. Asian Society of Gynecologic
Oncology, Korean Society of Gynecologic
Oncology, and Japan Society of Gynecologic
Oncology

This is an Open Access article distributed
under the terms of the Creative Commons
Attribution Non-Commercial License (<https://creativecommons.org/licenses/by-nc/4.0/>)
which permits unrestricted non-commercial
use, distribution, and reproduction in any
medium, provided the original work is properly
cited.

ORCID iDs

Chi-Son Chang 
<https://orcid.org/0000-0002-0169-2008>
Ji-Yoon Ryu 
<https://orcid.org/0000-0002-2655-7822>
June-Kuk Choi 
<https://orcid.org/0000-0003-0995-1622>
Young-Jae Cho 
<https://orcid.org/0000-0001-6181-9667>
Jung-Joo Choi 
<https://orcid.org/0000-0001-8620-2129>

¹Department of Obstetrics and Gynecology, Samsung Medical Center, Sungkyunkwan University School of Medicine, Seoul, Korea

²Research Institute for Future Medicine, Samsung Medical Center, Sungkyunkwan University School of Medicine, Seoul, Korea

³Department of Obstetrics and Gynecology, Uijeongbu Eulji Medical Center, Eulji University, Uijeongbu, Korea

⁴Department of Immunology, School of Medicine, Konkuk University, Chungju, Korea

⁵Innovative Discovery Center, Prestige Biopharma Korea, Busan, Korea

⁶Samsung Advanced Institute for Health Sciences & Technology, Sungkyunkwan University School of Medicine, Seoul, Korea

ABSTRACT

Objective: Fenbendazole (FZ) has potential anti-cancer effects, but its poor water solubility limits its use for cancer therapy. In this study, we investigated the anti-cancer effect of FZ with different drug delivery methods on epithelial ovarian cancer (EOC) in both in vitro and in vivo models.

Methods: EOC cell lines were treated with FZ and cell proliferation was assessed. The effect of FZ on tumor growth in cell line xenograft mouse model of EOC was examined according to the delivery route, including oral and intraperitoneal administration. To improve the systemic delivery of FZ by converting fat-soluble drugs to hydrophilic, we prepared FZ-encapsulated poly(D,L-lactide-co-glycolide) acid (PLGA) nanoparticles (FZ-PLGA-NPs). We investigated the preclinical efficacy of FZ-PLGA-NPs by analyzing cell proliferation, apoptosis, and in vivo models including cell lines and patient-derived xenograft (PDX) of EOC.

Results: FZ significantly decreased cell proliferation of both chemosensitive and chemoresistant EOC cells. However, in cell line xenograft mouse models, there was no effect of oral FZ treatment on tumor reduction. When administered intraperitoneally, FZ was not absorbed but aggregated in the intraperitoneal space. We synthesized FZ-PLGA-NPs to obtain water solubility and enhance drug absorption. FZ-PLGA-NPs significantly decreased cell proliferation in EOC cell lines. Intravenous injection of FZ-PLGA-NP in xenograft mouse models with HeyA8 and HeyA8-MDR significantly reduced tumor weight compared to the control group. FZ-PLGA-NPs showed anti-cancer effects in PDX model as well.

Conclusion: FZ-incorporated PLGA nanoparticles exerted significant anti-cancer effects in EOC cells and xenograft models including PDX. These results warrant further investigation in clinical trials.

Keywords: Fenbendazole; Epithelial Ovarian Cancer; PLGA Nanoparticle; Patient-Derived Xenograft; Drug Repurposing

Jae Ryoung Hwang 
<https://orcid.org/0000-0003-2319-5878>
 Ju-Yeon Choi 
<https://orcid.org/0000-0002-9112-5436>
 Joseph J. Noh 
<https://orcid.org/0000-0002-3132-8709>
 Chan Mi Lee 
<https://orcid.org/0000-0002-3301-6733>
 Ji Eun Won 
<https://orcid.org/0000-0003-1946-2435>
 Hee Dong Han 
<https://orcid.org/0000-0002-3300-5575>
 Jeong-Won Lee 
<https://orcid.org/0000-0002-6110-4909>

Funding

This work was supported by the Korea Medical Device Development Fund grant funded by the Korean government (Ministry of Science and ICT [MSIT], Ministry of Trade, Industry, and Energy, Ministry of Health & Welfare, Ministry of Food and Drug Safety) (KMDF_PR_20200901_0153-2022) and the National Research Foundation of Korea (NRF) grant funded by the Korean government (MSIT) (2020R1C1C1007482).

Conflict of Interest

No potential conflict of interest relevant to this article was reported.

Data Availability Statement

The data generated in this study are available upon request from the corresponding author.

Author Contributions

Conceptualization: L.J.W.; Data curation: C.Y.J.; Formal analysis: C.C.S.; Investigation: R.J.Y., C.Y.J., H.J.R., L.C.M., W.J.E.; Methodology: H.J.R., C.J.Y., N.J.J., H.H.D.; Resources: C.J.J.; Supervision: C.J.K., L.J.W.; Visualization: R.J.Y.; Writing - original draft: C.C.S.; Writing - review & editing: R.J.Y., H.H.D., L.J.W.

Synopsis

We developed fenbendazole-encapsulated PLGA nanoparticles (FZ-PLGA-NPs) in water-soluble form, showing anti-cancer effect on epithelial ovarian cancer (EOC) cells in vitro and in vivo. FZ-PLGA-NPs enabled the systemic delivery of FZ with improved cytotoxic effects in cell line xenograft and patient-derived xenograft mouse models of EOC.

INTRODUCTION

Epithelial ovarian cancer (EOC) is the second most common and leading cause of mortality among all gynecologic malignancies [1]. In addition to the standard treatment of primary cytoreductive surgery followed by platinum-based combination chemotherapy, due to recent advances in treatment modalities, bevacizumab and poly (ADP-ribose) polymerase inhibitor are being widely used in therapeutic and maintenance settings [2]. Despite a good response to primary treatment, most patients with advanced disease experience relapse and eventually die from the disease [3]. Patients with advanced EOC have a 5-year survival of only 40% [4], and there is an unmet need to find new therapeutic drugs for EOC.

Drug repurposing has become a promising option for finding new anti-cancer drugs at lower costs and in shorter times. Fenbendazole (FZ), a widely used benzimidazole anthelmintic drug for treating gastrointestinal parasites, has recently been shown to have anti-cancer effects against several cancer types [5-7]. Furthermore, it has been reported that benzimidazole anthelmintics exhibited anti-cancer effects in paclitaxel and doxorubicin-resistant cancer cells [8,9]. The suggested mechanisms of its antitumor effects are the disruption of microtubule polymerization, G2/M phase cell cycle arrest, and anti-angiogenesis [10]. Especially in ovarian cancer models, the potential anti-vascular endothelial growth factor (VEGF) activity of benzimidazole analogs has been reported, showing the inhibition of peritoneal tumor growth and ascites formation through intraperitoneal (IP) administration [11-13].

However, FZ and its analogs have low water solubility and poor bioavailability [14], which are major obstacles to its clinical application as an anti-cancer agent. Drug delivery with nanoparticles has been recently proposed to overcome some of the challenges of drug delivery. Several nanoparticle platforms have been developed to enhance drug delivery [15]. Poly(D,L-lactide-co-glycolide) acid (PLGA) polymer is a suitable option for clinical and biological applications owing to its low toxicity, biocompatibility, biodegradability, and low immunogenicity [16]. Taking this into consideration, we utilized PLGA as the polymeric matrix and developed a method of encapsulating FZ in PLGA-nanoparticles to increase the hydrophilicity of FZ.

In this study, we aimed to investigate the anti-cancer effect of FZ on EOC models by conducting in vitro and in vivo experiments. We also aimed to explore the anti-cancer effect of FZ with different drug delivery modes on EOC using natural FZ and FZ-encapsulated PLGA-nanoparticles (FZ-PLGA-NPs).

MATERIALS AND METHODS

1. Cell lines and materials

Human EOC cell lines (HeyA8, SKOV3ip1, A2780-CP20, HeyA8-MDR and SKOV3-TR) were a gift from Dr. Anil K. Sood, Department of Cancer Biology, University of Texas M.D. Anderson Cancer Center, Houston, TX, USA. A2780 cells were purchased from the European Collection of Authenticated Cell Cultures (Cat No.93112520). All ovarian cancer cells were maintained in RPMI 1640 supplemented with 10% fetal bovine serum, and all cells were maintained in 5% CO₂ at 37°C. FZ, PLGA (Resomer RG502H, monomer ratio 50:50, MW 7–17 kDa), and poly(vinyl alcohol) (PVA, 80% hydrolyzed, MW 9–10 kDa) were purchased from Sigma-Aldrich (St. Louis, MO, USA). FZ was resuspended in dimethyl sulfoxide (DMSO) at a concentration of 5 mg/mL.

2. Preparation of FZ-PLGA-NPs

We prepared FZ-PLGA-NPs by an oil-in-water emulsion method [17]. Briefly, 20 mg of FZ was dissolved in 2 mL of DMSO and mixed with 2 mL of chloroform containing 80 mg of PLGA as the oil phase. The oil phase was mixed with 10 mL of a 2.0% (w/v) PVA solution using a probe-type sonicator (SONICS, Newtown, CT, USA) at 4°C for 10 minutes (40 pulses of 5 seconds with 3-second gap). Chloroform and DMSO in the emulsion were evaporated using a rotary evaporator at 30°C under a vacuum. After evaporation, FZ-PLGA-NPs were washed thrice by centrifugation at 13,000 rpm for 20 minutes and stored at 4°C until use. The size and zeta potential of the FZ-PLGA-NPs were measured by dynamic light scattering using an electrophoretic light scattering photometer (SZ-100; Horiba, Kyoto, Japan) [18]. The loading efficiency of FZ in the FZ-PLGA-NPs was measured by a UV-vis spectrophotometer (UV-mini; Shimadzu, Kyoto, Japan) at a wavelength of 285 nm [19].

3. Cell proliferation assay

Cells were plated in the culture medium in a 96-well plate at 3×10³ cells/well. After 24 hours, the cells were treated with FZ or FZ-PLGA-NPs and the assay was performed at 24, 48, and 72 hours. For proliferation assays, the cells were stained with 3-(4,5-dimethylthiazol-2-yl)-2,5-diphenyltetrazolium bromide (MTT; Amresco, Solon, OH, USA). After 4 hours of additional incubation, the medium was discarded, 100 µL of acidic isopropanol (0.1 N HCL in absolute isopropanol) was added, and the plate was shaken gently. Absorbance was measured on an enzyme-linked immunosorbent assay reader at a test wavelength of 540 nm.

4. Apoptosis assay

Cell apoptosis was measured at 48 hours using the Annexin V-FITC Apoptosis Detection Kit-1 (BD Pharmingen, San Diego, CA, USA) according to the manufacturer's protocol. Briefly, cells were washed twice in phosphate-buffered saline and the pellet was resuspended in annexin V binding buffer at a concentration of 10⁶ cells/mL. Annexin V FITC and propidium iodide were added (5 µL to each per 10⁵ cells). The samples were gently mixed and incubated for 15 minutes at room temperature in the dark before fluorescence-activated cell sorter (FACS) analysis.

5. Western blot analysis

Cells were lysed in PRO-PRE Protein Extraction Solution (Intron Biotechnology, Seongnam, Korea). Protein concentrations were analyzed using a Bradford assay kit (Bio-Rad, Hercules, CA, USA). Cells (40 µg of total protein) were separated on 7.5% or 10% acrylamide gels by sodium dodecyl sulfate-polyacrylamide gel electrophoresis and transferred to Immobilon-P transfer membranes (Merck Millipore, Burlington, MA, USA).

Membranes were blocked for 1 hour with 5% skim milk in Tris-buffered saline containing 0.1% Tween-20 at room temperature. The protein bands were probed with total-PI3K and phospho-PI3K, total-AKT and phospho-AKT (p-AKT), total-mTOR and phospho-mTOR (p-mTOR), and total-ERK and phospho-ERK (p-ERK) (Cell Signaling Technology, Danvers, MA, USA) antibodies at 1:1,000 dilutions or with total-S6K1 and phospho-S6K1 (p-S6K1), and β -actin (Santa Cruz Biotechnology, Dallas, TX, USA) antibodies at a 1:2,000 dilution and then tagged with horseradish peroxidase-conjugated anti-rabbit antibody (GE Healthcare, Piscataway, NJ, USA). Bands were envisioned by enhanced chemiluminescence using an ECL kit (Amersham Biosciences, Buckinghamshire, UK) according to the manufacturer's protocol.

6. Immunohistochemistry

Immunohistochemical studies were performed on formalin-fixed, paraffin-embedded, 4- μ m-thick tissue sections. Immunostaining for Ki-67 (NB600-1252; NOVUS Biologicals, Centennial, CO, USA) was performed with a BOND-MAX™ automated immunostaining device (Leica Biosystems, Melbourne, Australia) and the Bond™ Polymer purification detection kit (Vision Biosystems, Melbourne, Australia). Briefly, antigen retrieval was carried out in ER1 buffer at 97°C for 20 minutes. Endogenous peroxidase activity was blocked with 3% hydrogen peroxidase for 10 minutes, and the antibody was diluted at room temperature at 1:200 for 15 minutes. Apoptotic-positive cells were analyzed by the TUNEL assay using the ApopTag Peroxidase In Situ Apoptosis Detection Kit (Merck Millipore) as described above.

7. Animal care and orthotopic implantation of tumor cells

Female BALB/c nude mice were purchased from Orient Bio, Seongnam, Korea. This study was reviewed and approved by the Institutional Animal Care and Use Committee of the Samsung Biomedical Research Institute (protocol No. H-A9-003), which is accredited by the Association for the Assessment and Accreditation of Laboratory Animal Care International and abides by the guidelines of the Institute of Laboratory Animal Resources (ILAR).

The mice used in these experiments were 6 to 8 weeks old. To establish orthotopic models, HeyA8 (2.5×10^5 cells/0.2 mL Hanks' Balanced Salt Solution [HBSS]) and HeyA8-MDR (1×10^6 cells/0.2 mL HBSS) cells were injected into the peritoneal cavity of the mice. For the patient-derived xenograft (PDX) model of EOC, a specimen of the patient's tumor collected in the operating room was cut to less than 2–3 mm and transplanted into the subrenal capsule of the left kidney of a mouse by continuous transplantation [20,21]. We selected a PDX from a 53-year-old woman with International Federation of Gynecology and Obstetrics stage IIIC and high-grade serous histology ovarian cancer. She was treated with primary cytoreductive surgery followed by 6 cycles of paclitaxel-carboplatin combination chemotherapy. There was no residual tumor after primary surgery, and her progression-free survival was 45 months.

FZ was orally or intraperitoneally administered (3 times/week). FZ-PLGA-NPs (1 mg/mouse) were intravenously injected (3 times/week). The mice (n=10 per group) were monitored daily for tumor development and were euthanized on days 21 – 28 after the injection of cancer cells, on days 70 – 85 (PDX model), or when considered moribund. Total body weight and tumor weight were recorded at the time of euthanization. Tumors were fixed in formalin and embedded in paraffin or snap-frozen in OCT compound (Sakura Finetek Japan, Tokyo, Japan) in liquid nitrogen.

8. Statistical analysis

The Mann-Whitney U test was used to evaluate the significance and to compare differences among the groups for both in vitro and in vivo assays using a statistical software package (Prism; GraphPad, San Diego, CA, USA). The p-values of less than 0.05 were considered statistically significant.

RESULTS

1. Effect of natural FZ on the cell viability of EOC cells

We first confirmed the in vitro anti-cancer effect of FZ in EOC cell lines. We performed the MTT assay to investigate whether the natural form of FZ inhibited the proliferation of EOC cells (**Fig. 1**). The results showed that treatment with FZ significantly decreased the cell viability of chemosensitive (A2780, HeyA8, SKOV3ip1) EOC cells in a dose-dependent manner at 24 hours. In chemoresistant EOC cells, FZ significantly reduced cell viability in A2780-CP20 and HeyA8-MDR cells, but not SKOV3-TR cells. When we extended the exposure time of FZ to 48 hours, a significant reduction in cell proliferation was observed in all EOC cell lines by treatment with FZ. Similar results were observed when the exposure time was extended to 72 hours. The half-maximal inhibitory concentration (IC₅₀) values ranged from 0.32 μM to 1.01 μM for natural FZ, with SKOV3-TR cell line exhibiting the least sensitivity (**Table S1**).

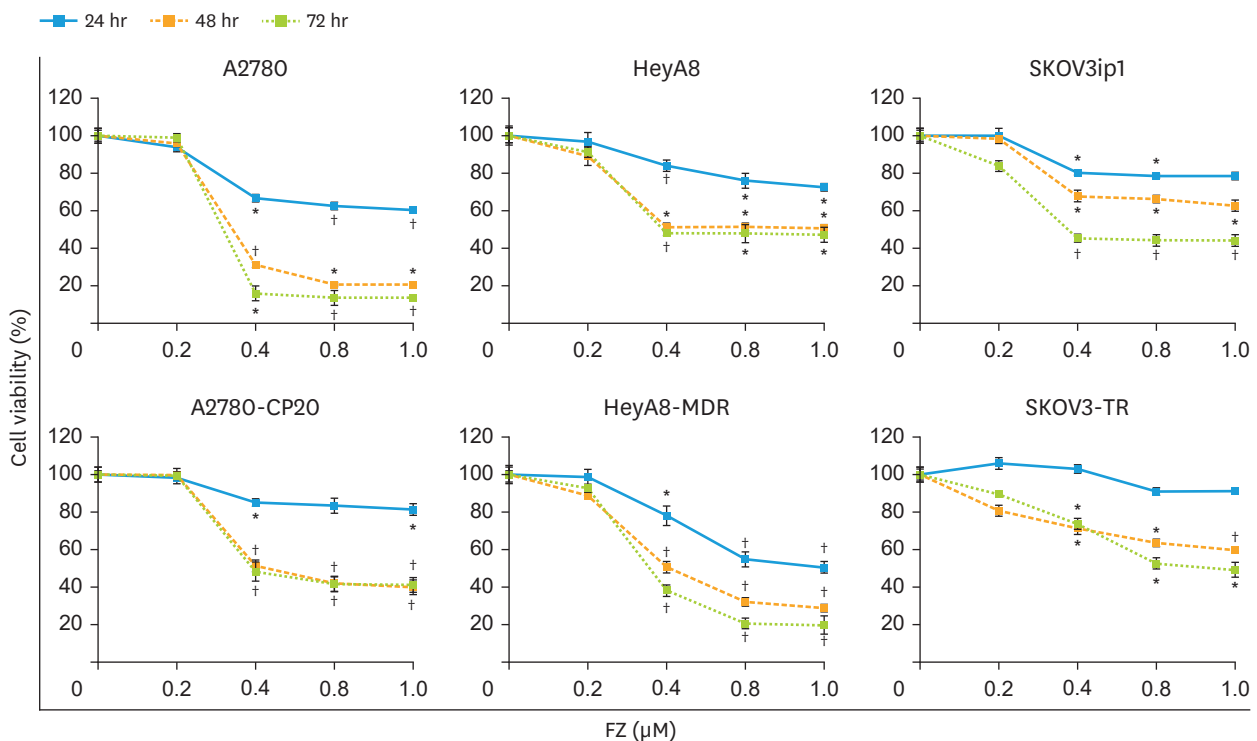


Fig. 1. Cell proliferation following treatment of epithelial ovarian cancer cells with natural FZ. FZ inhibited cell proliferation in a dose-dependent manner, as evaluated by the 3-(4,5-dimethylthiazol-2-yl)-2,5-diphenyltetrazolium bromide assay. All experiments were repeated 3 times. Error bars represent the standard error of the mean. FZ, fenbendazole. *p<0.05; †p<0.001.

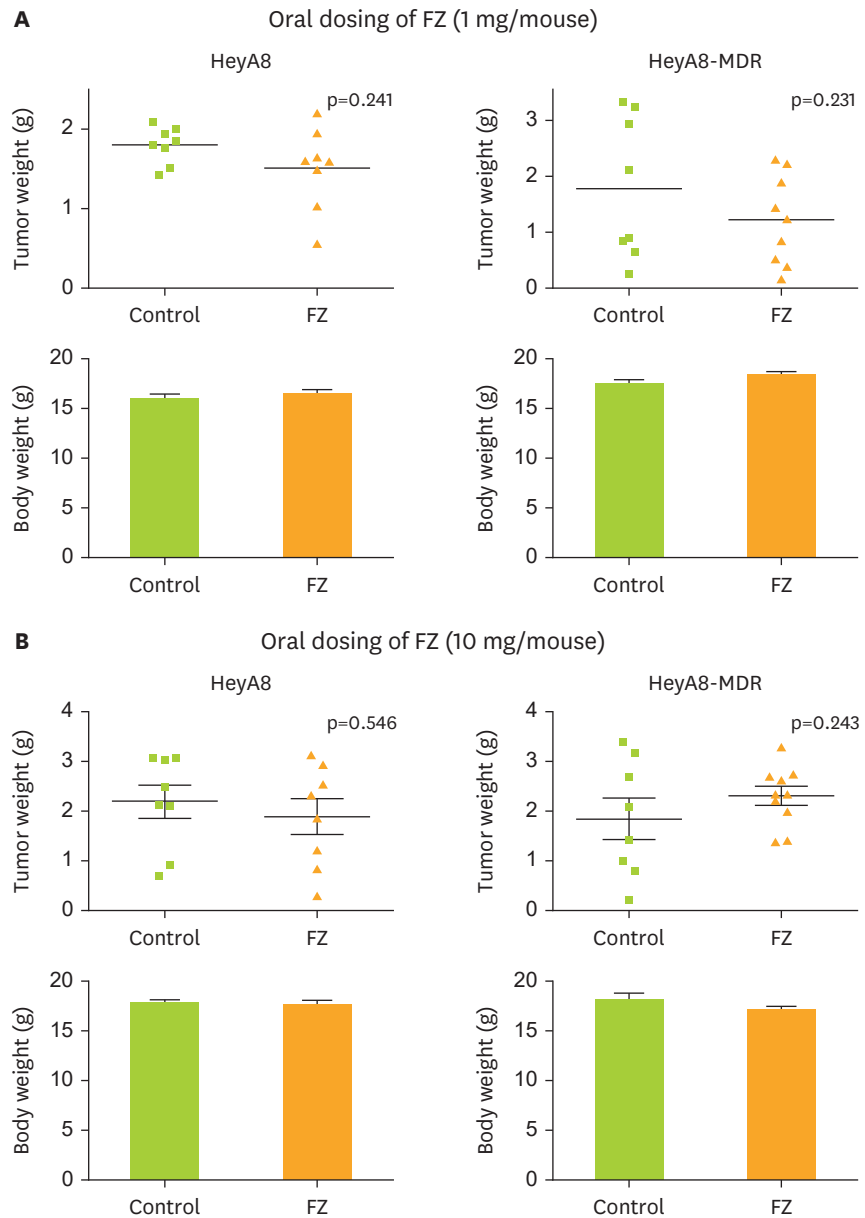


Fig. 2. In vivo efficacy of treatment with natural FZ in the cell-line xenograft model of epithelial ovarian cancer. Oral administration of (A) 1 mg and (B) 10 mg of natural FZ did not reduce the tumor weight in either HeyA8 or HeyA8-MDR model. FZ, fenbendazole.

2. In vivo efficacy of natural FZ in xenograft mouse models for EOC

We next investigated the efficacy of FZ on tumor growth in vivo using the cell line xenograft mouse model for EOC. HeyA8 and HeyA8-MDR cells were implanted into the peritoneal cavity of female nude mice. HeyA8 and HeyA8-MDR model mice treated with a 1 mg dose of natural FZ did not show reductions in tumor weight (**Fig. 2A**). Likewise, no tumor reduction was observed when the dose of FZ was increased to 10 mg (**Fig. 2B**).

Since FZ has low systemic bioavailability due to extensive first-pass metabolism when administered orally [22], the drug administration route was changed to IP injection.

However, FZ was observed to aggregate in the IP cavity of the mice and was not absorbed (**Fig. S1**). Based on these results, we concluded that FZ in natural form could not be delivered to the tumor cells *in vivo* due to its low water solubility.

3. Characteristics of FZ-PLGA-NPs and effect on cell proliferation and apoptosis

We utilized PLGA as a polymeric matrix and prepared FZ-PLGA-NPs encapsulating FZ to enhance the water solubility and absorption of FZ. We first determined the physical properties of FZ-PLGA-NPs (**Fig. 3**). The mean particle size and zeta potential were 531 ± 5.31 nm and -30.6 ± 1.36 mV, respectively (**Fig. 3A and B**). FZ-PLGA-NPs had increased particle size due to FZ encapsulation. A representative histogram of the PLGA-NPs and FZ-PLGA-NPs is shown in **Fig. 3C**, which indicates the size distribution of the NPs. The loading efficiency of FZ in FZ-PLGA-NPs was 89% (**Fig. 3D**).

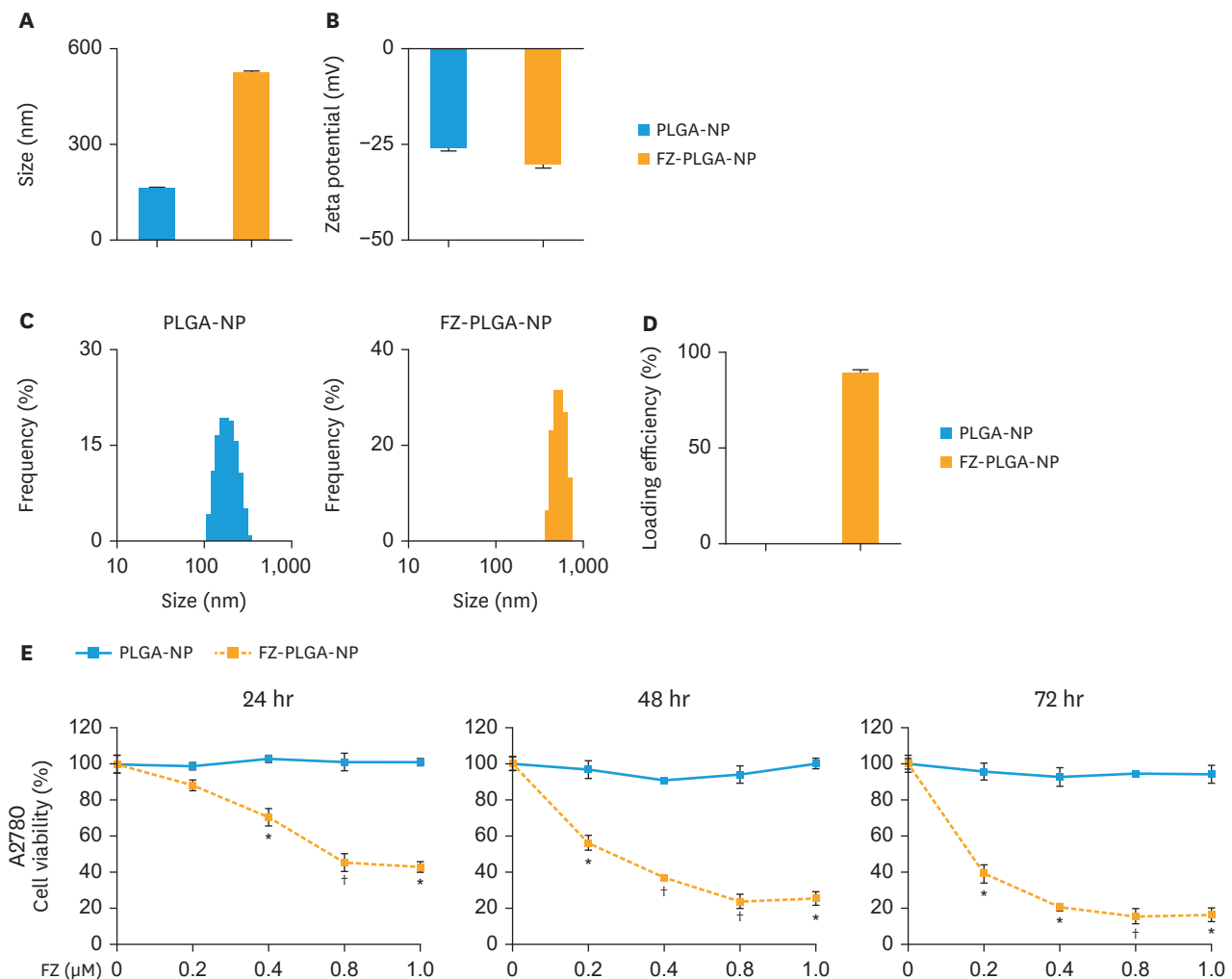


Fig. 3. Physical properties of FZ-PLGA-NPs. (A) Size, (B) surface charge, and (C) size distribution histogram of PLGA-NPs and FZ-PLGA-NPs. FZ-PLGA-NPs have increased particle size due to FZ encapsulation. (D) The loading efficiency of FZ into PLGA-NPs was 89%. (E) Cell proliferation following treatment of epithelial ovarian cancer cells with PLGA-NPs and FZ-PLGA-NPs was assessed via the 3-(4,5-dimethylthiazol-2-yl)-2,5-diphenyltetrazolium bromide assay. PLGA-NPs did not show cytotoxicity, whereas FZ-PLGA-NPs inhibited cell proliferation in dose- and time-dependent manners. Error bars represent the standard error of the mean. FZ, fenbendazole; FZ-PLGA-NP, fenbendazole-encapsulated poly(D,L-lactide-co-glycolide) acid nanoparticle; PLGA-NP, poly(D,L-lactide-co-glycolide) acid nanoparticle. * $p < 0.05$; † $p < 0.001$.

(continued to the next page)

FZ-PLGA-NP in ovarian cancer

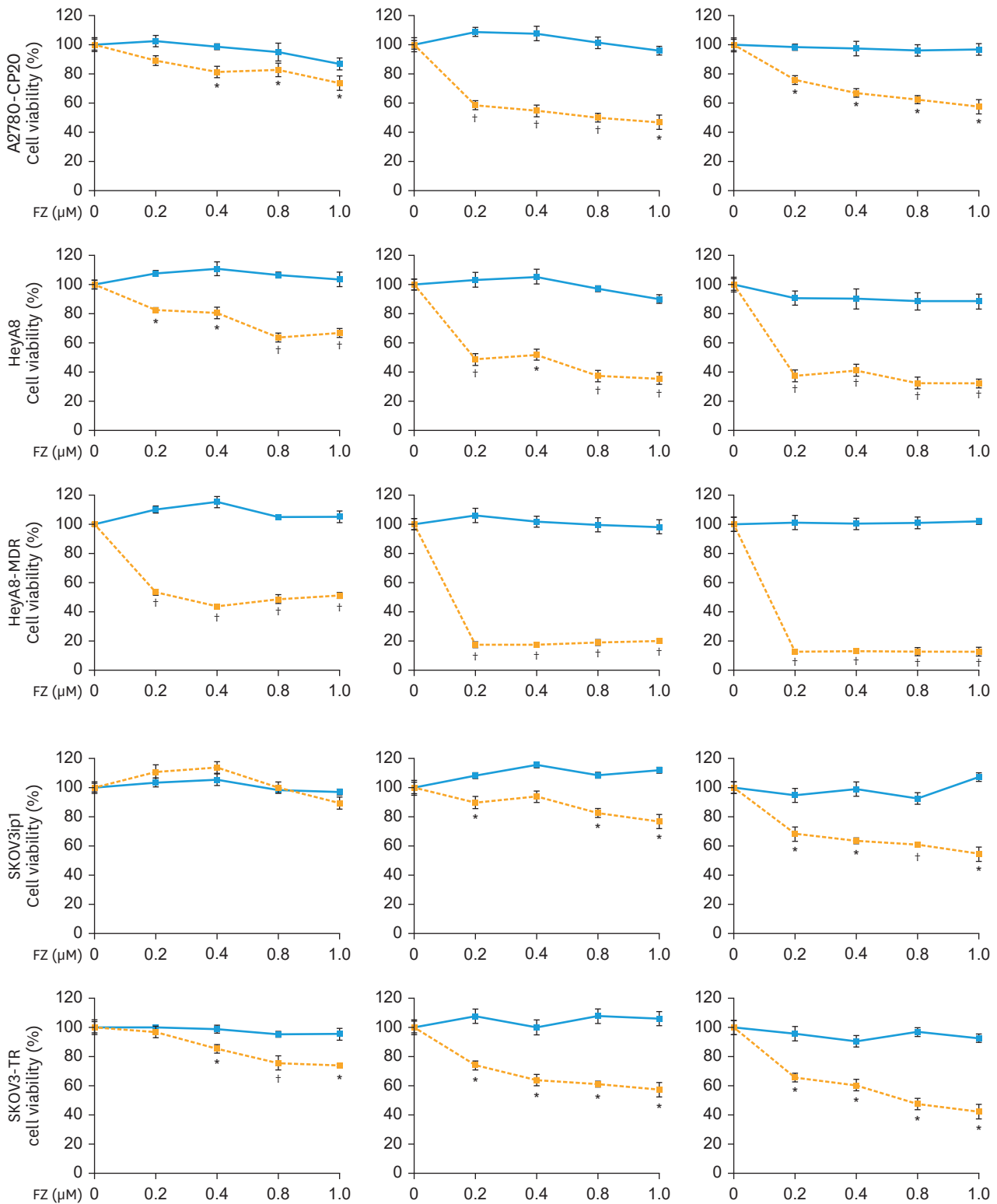


Fig. 3. (Continued) Physical properties of FZ-PLGA-NPs. (A) Size, (B) surface charge, and (C) size distribution histogram of PLGA-NPs and FZ-PLGA-NPs. FZ-PLGA-NPs have increased particle size due to FZ encapsulation. (D) The loading efficiency of FZ into PLGA-NPs was 89%. (E) Cell proliferation following treatment of epithelial ovarian cancer cells with PLGA-NPs and FZ-PLGA-NPs was assessed via the 3-(4,5-dimethylthiazol-2-yl)-2,5-diphenyltetrazolium bromide assay. PLGA-NPs did not show cytotoxicity, whereas FZ-PLGA-NPs inhibited cell proliferation in dose- and time-dependent manners. Error bars represent the standard error of the mean. FZ, fenbendazole; FZ-PLGA-NP, fenbendazole-encapsulated poly(D,L-lactide-co-glycolide) acid nanoparticle; PLGA-NP, poly(D,L-lactide-co-glycolide) acid nanoparticle. * $p < 0.05$; † $p < 0.001$.

Next, we assessed the cytotoxic effect of FZ-PLGA-NPs and compared it to that of PLGA-NPs without encapsulation of FZ. Control PLGA-NPs did not show cytotoxic effects in any of the EOC cell lines. In contrast, treatment with FZ-PLGA-NPs significantly decreased the cell viability of chemosensitive and chemoresistant EOC cells (**Fig. 3E**), similar to the MTT assay results with natural FZ. The IC_{50} values ranged from 0.12 μ M to 0.81 μ M for FZ-PLGA-NPs, with SKOV3ip1 and SKOV3-TR cell lines exhibiting the least sensitivity (**Table S2**). SKOV3ip1 cell line treated with FZ-PLGA-NPs did not reach 50% viability relative to the control. The EOC cell lines that showed the best sensitivity were HeyA8 and HeyA8-MDR.

FACS analysis of EOC cells was performed using FZ-PLGA-NPs containing 1 μ M of FZ to assess apoptosis. Apoptotic cells were measured by annexin V incorporation after treatment with FZ-PLGA-NPs, and the results were similar to those from the cell proliferation assay. The proportion of apoptotic cells was significantly increased in A2780, A2780-CP20, HeyA8, HeyA8-MDR, SKOV3ip1, and SKOV3-TR cells 48 hours after treatment with FZ-PLGA-NPs (**Fig. 4**).

4. In vivo efficacy of FZ-PLGA-NPs in mouse xenograft models including PDX

To confirm the anti-cancer effect of FZ-PLGA-NPs seen in the in vitro results, we performed in vivo experiments using EOC cell line xenografts and PDX models. FZ-PLGA-NPs were administered to the mice intravenously as the formula was hydrophilic. In both HeyA8 and HeyA8-MDR models, treatment with FZ-PLGA-NPs resulted in significant inhibition of tumor growth compared to the controls treated with PLGA-NPs (**Fig. 5A**). When applied to the PDX model, tumor weight and size after treatment with FZ-PLGA-NPs were significantly reduced compared to the controls (**Fig. 5B**). The body weight of the mice that received FZ-PLGA-NPs did not differ compared with those who received the control treatment (PLGA-NP). Using the harvested tumor tissue, we also confirmed the inhibiting effect of this treatment; Ki-67, a cell proliferation marker, was significantly decreased after treatment, whereas TUNEL, a marker of apoptosis, was significantly increased. Consistent results were observed in mouse models using HeyA8 and HeyA8-MDR cells, as well as in the PDX model.

5. Potential mechanism for the anti-cancer effect of FZ-PLGA-NPs in EOC cells

FZ decreases the activation of mTOR and several MAPK members, which are involved in the regulation of cell survival and apoptosis, depending upon the cell type [23,24]. To identify the effect of FZ in regulating cell proliferation or apoptosis, we evaluated the PI3K/mTOR pathway in EOC cells by Western blot analysis. Following the treatment of HeyA8 and HeyA8-MDR cells with FZ-PLGA-NPs, the expression of p-mTOR, p-S6K1, p-AKT, and p-ERK significantly decreased compared to the control cells (**Fig. 6**). These changes in protein expression were not observed when only the carrier polymer PLGA-NP was administered. These results suggest that FZ modulated cell proliferation by inhibiting the PI3K/mTOR signaling pathway in EOC cells.

DISCUSSION

In this study, we developed a drug delivery carrier system (FZ-PLGA-NPs) to overcome the water insolubility of FZ in applications for cancer therapy. In addition, FZ-PLGA-NPs significantly showed anti-cancer effects on cell proliferation and apoptosis in EOC cells. We also confirmed that FZ-PLGA-NPs significantly inhibited tumor growth in cell line xenograft and PDX models.

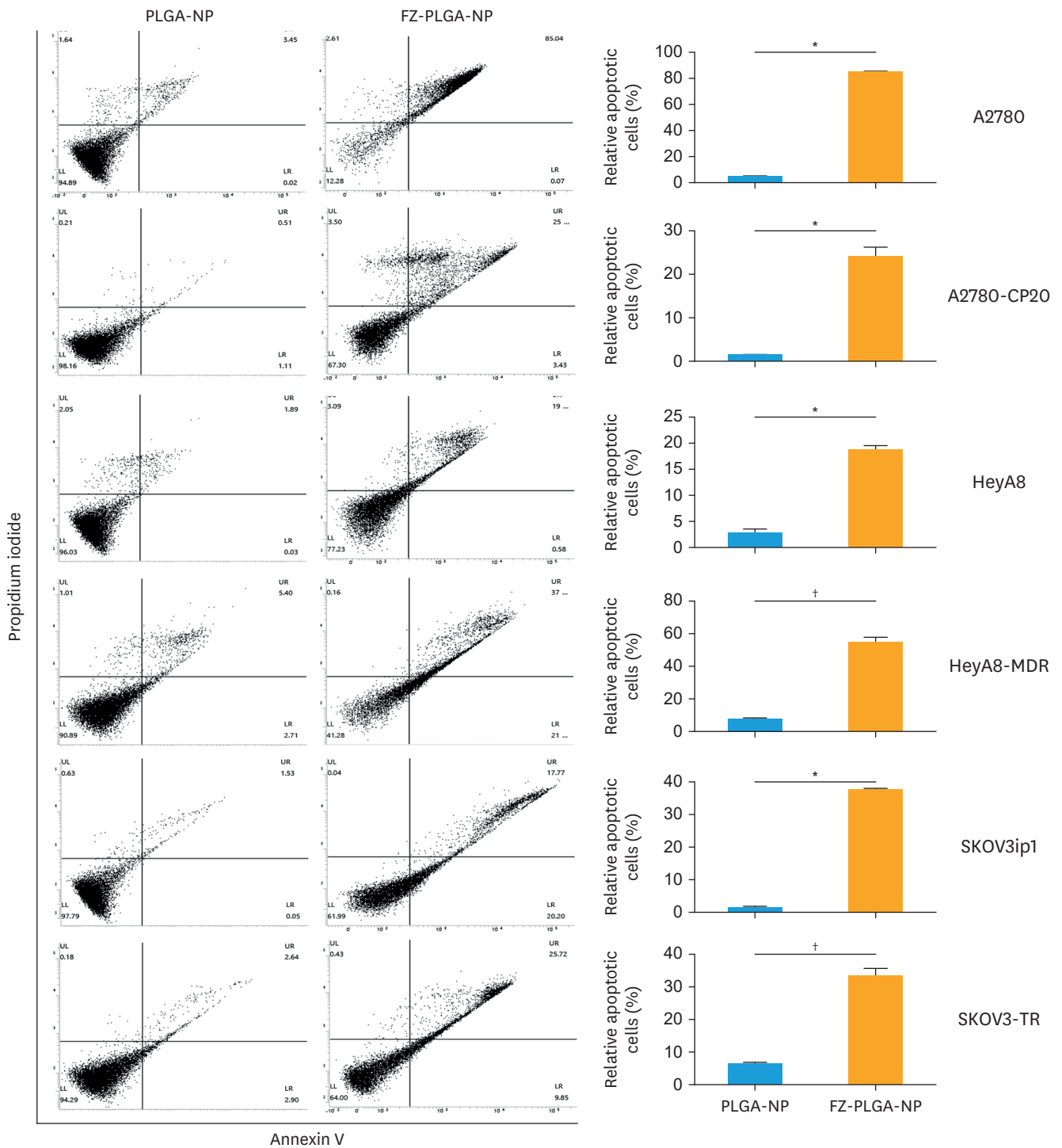


Fig. 4. Apoptosis assay of EOC cells treated with PLGA-NPs and FZ-PLGA-NPs. Apoptotic cell death was measured by fluorescence-activated cell sorter analysis detecting annexin V after 48 hours of treatment. In all EOC cells, the apoptotic population significantly increased after treatment with FZ-PLGA-NPs. Error bars represents the standard error of the mean.

EOC, epithelial ovarian cancer; FZ-PLGA-NP, fenbendazole-encapsulated poly(D,L-lactide-co-glycolide) acid nanoparticle; PLGA-NP, poly(D,L-lactide-co-glycolide) acid nanoparticle.

* $p < 0.05$; † $p < 0.001$.

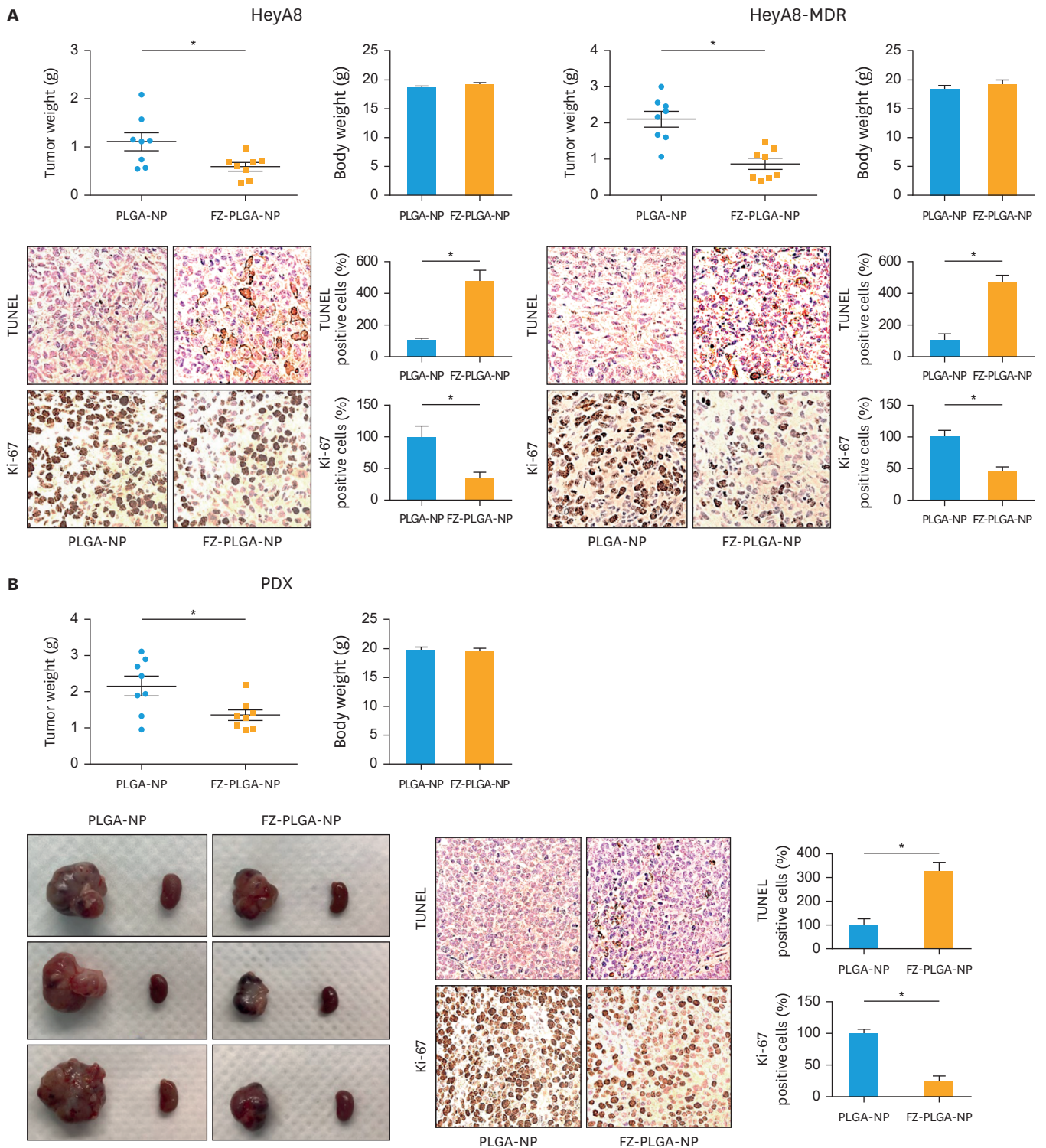


Fig. 5. In vivo efficacy of treatment with FZ-PLGA-NPs in cell line xenograft and PDX models of EOC. (A) In cell line xenograft models using HeyA8 and HeyA8-MDR cells, treatment with FZ-PLGA-NPs significantly inhibited tumor growth compared to the controls treated with PLGA-NPs. The body weight of the mice that received FZ-PLGA-NPs did not differ compared to those who received the control treatment. Tumor cell proliferation based on Ki-67 immunohistochemical analysis of harvested tumor tissues was significantly decreased in the FZ-PLGA-NP group. Conversely, the TUNEL assay showed higher apoptosis in the FZ-PLGA-NP group. (B) Consistent results were observed in the PDX mouse model. Tumor weight and size after treatment with FZ-PLGA-NPs were significantly reduced compared to the control treatment. FZ-PLGA-NP, fenbendazole-encapsulated poly(D,L-lactide-co-glycolide) acid nanoparticle; PDX, patient-derived xenograft; PLGA-NP, poly(D,L-lactide-co-glycolide) acid nanoparticle. * $p < 0.05$.

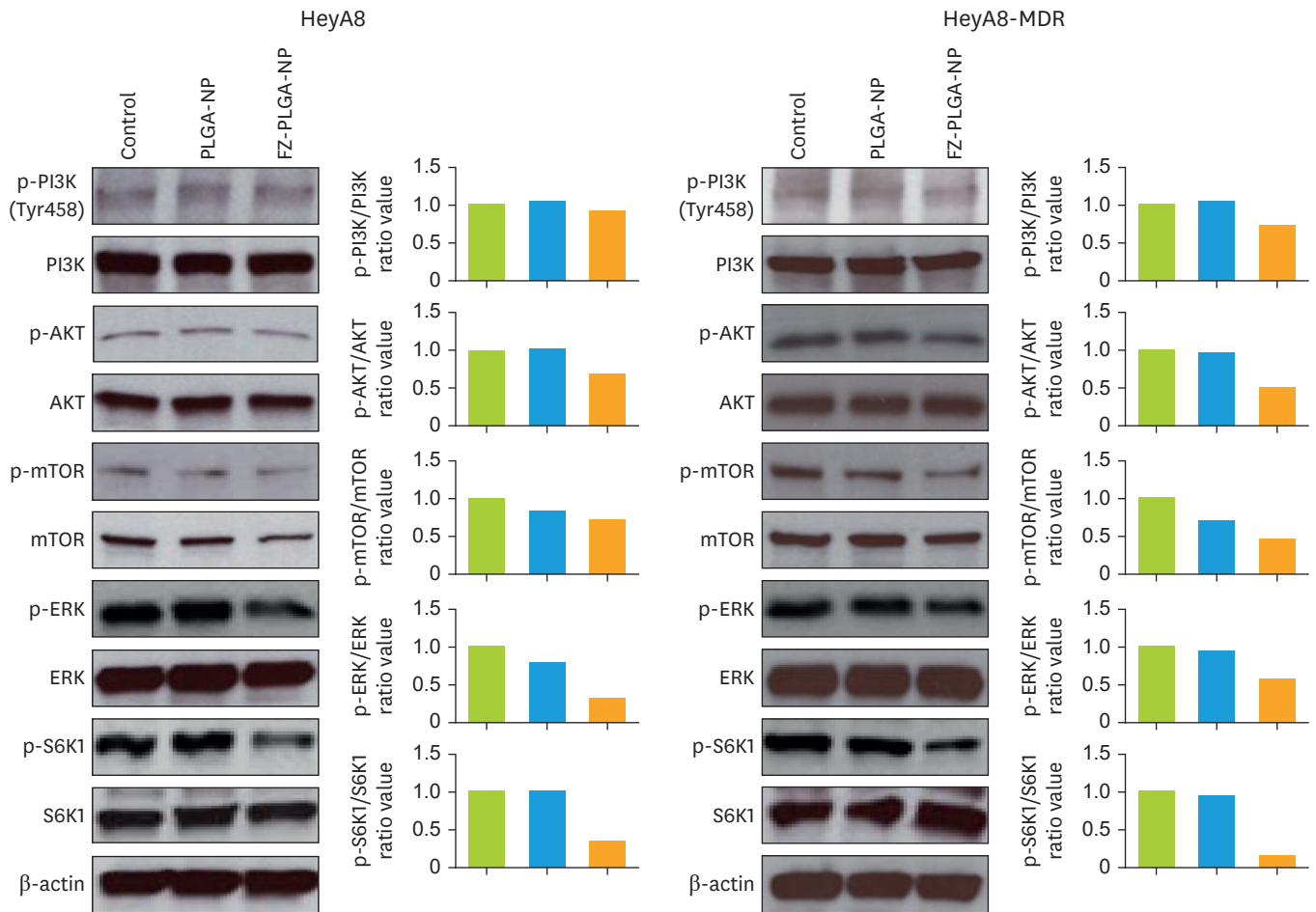


Fig. 6. Analysis of the FZ mediated PI3K/mTOR pathway in epithelial ovarian cancer cells. Cells were incubated with dimethyl sulfoxide (control), PLGA-NPs or FZ-PLGA-NPs (1 μ M) for 1 hour, harvested and subjected to Western blot analysis of p-PI3K, p-AKT, p-mTOR, p-ERK and p-S6K1 levels. FZ-PLGA-NP, fenbendazole-encapsulated poly(D,L-lactide-co-glycolide) acid nanoparticle; p-, phospho-; PLGA-NP, poly(D,L-lactide-co-glycolide) acid nanoparticle.

Recently, a video of a terminal stage lung cancer patient in US claiming to have been cured after taking FZ gained a lot of attention online. Since then, there have been cases of cancer patients recklessly purchasing and taking anthelmintic agents including FZ on their own. FZ and benzimidazole anthelmintic agents have been known to exhibit anti-cancer effects in vitro [5-13], but there is limited in vivo data, and there is even less data on human use so far. This study showed that oral administration of the natural form of FZ has no anti-cancer effect in vivo, suggesting a scientific evidence against self-administration of FZ by cancer patients. The anti-cancer effect of FZ was seen in vivo only in water-soluble form of FZ-PLGA-NPs.

Benzimidazole anthelmintics have been explored as anti-cancer drugs for drug repurposing. They have been shown to inhibit cell viability in a variety of cancer cell lines, including colorectal, liver, lung, and brain tumors [25-28]. In ovarian cancer models, the main anti-cancer mechanism proven was anti-angiogenesis through the down-regulation of VEGF [11-13]. The traditional mechanism of action of FZ is microtubule destabilization [7], and several broadly used anti-cancer drugs, including paclitaxel, induce their effects by perturbing microtubule dynamics [9]. In this study, FZ-PLGA-NPs were effective on paclitaxel-resistant EOC cells as well as paclitaxel-sensitive EOC cells. This study demonstrated the anti-cancer mechanism of FZ in ovarian cancer models, where FZ affected cell proliferation and apoptosis

by inhibiting the PI3K/mTOR signaling pathway. The PI3K/mTOR pathway is a growth-regulating cellular signaling pathway that plays a significant role in cell survival and anti-apoptotic mechanisms in cancer [29]. Treatment with FZ-PLGA-NPs significantly decreased the phosphorylation of AKT, ERK, and S6K1, which are downstream proteins of the PI3K/mTOR pathway.

Previous reports in ovarian cancer animal models demonstrated the anti-tumor effect of the IP administration of albendazole, but the drug dose was very high, ranging from 150 mg/kg to 450 mg/kg [11-13], whereas the acceptable dose for the human use of albendazole is up to 400 mg per day [10]. Due to its low water solubility and bioavailability, it must have been used at such a high dose to exhibit a cytotoxic effect. However, the dose was so high that it could be expected to be highly toxic when clinically applied. Therefore, various methods for increasing the solubility of benzimidazole anthelmintics have been proposed. Pourgholami et al. [30] and Pillai et al. [31] suggested attaching cyclodextrin, a cyclic oligosaccharide, to improve the poor aqueous solubility of albendazole. The next concept for improving water solubility was nanoparticle drug delivery systems. Albumin nanoparticles carrying albendazole were assembled and demonstrated anti-cancer effects in an EOC animal model at a much lower drug dose of 10 mg/kg [32]. In other cancer types, several other nanoparticles were developed to overcome the poor aqueous solubility of FZ in prostate cancer and glioma [33,34]. We utilized PLGA-NPs as a platform to deliver FZ effectively to EOC tumor cells, and successfully demonstrated anti-cancer effects with low toxicity in animal models. Although the pharmacokinetic properties of FZ is well established because of its long history of use [10], the pharmacokinetics of FZ-PLGA-NP employing nanoparticles may change due to increased water solubility. We did not perform pharmacokinetic evaluation, and this is a limitation of this study. Further studies on this aspect will be needed in the future for human use of the drug.

Nanoparticle systems are attractive systems that can carry a large payload of drugs compared to antibody conjugates [35]. Furthermore, drugs are located within the particles so that their pharmaceutical properties may not affect the distribution of the nanoparticles themselves [18]. Among various types of nanoparticle systems, PLGA-NPs are widely used for the targeted delivery of drugs due to their low toxicity and high biocompatibility [36]. Several studies have used PLGA-NPs for the targeted delivery of cisplatin or paclitaxel in drug-resistant ovarian cancer [37-39]. The attachment of targeting ligands, which enables particular interactions between the nanoparticles and the target cell surface, may play a key role in the delivery of nanoparticles. In our study, FZ-PLGA-NPs showed cytotoxic effects on EOC models using the paclitaxel-resistant HeyA8-MDR cell line, as well as in models with chemosensitive EOC cells. The targeted delivery of FZ-PLGA-NPs with an appropriate ligand might enhance anti-cancer effects in chemoresistant EOC. Also, utilization of other types of NP platforms and comparison of their efficacy should be considered, and further research is needed in this regard.

In conclusion, we demonstrated the anti-cancer effects of FZ in various drug delivery modes in EOC models. The natural form of FZ was effective in EOC cells *in vitro*, but neither oral nor IP administration *in vivo* had any effect due to the water insolubility of the drug. We combined FZ with PLGA-NPs for the first time. The anti-cancer effects of the water-soluble form of FZ-PLGA-NPs in EOC cells were identified both *in vitro* and *in vivo* including in PDX models. Further experiments and clinical trials should be considered in the future for the clinical use of FZ in ovarian cancer treatment.

SUPPLEMENTARY MATERIALS

Table S1

IC₅₀ values of natural fenbendazole for cell proliferation in epithelial ovarian cancer cell lines

[Click here to view](#)

Table S2

IC₅₀ values of FZ-PLGA-NP for cell proliferation in epithelial ovarian cancer cell lines

[Click here to view](#)

Fig. S1

IP administration of natural FZ in the cell line xenograft model of epithelial ovarian cancer. Red circles indicate aggregated FZ in the IP cavity of the mice.

[Click here to view](#)

REFERENCES

1. Siegel RL, Miller KD, Fuchs HE, Jemal A. Cancer statistics, 2022. *CA Cancer J Clin* 2022;72:7-33.
[PUBMED](#) | [CROSSREF](#)
2. Lee YY, Choi MC, Park JY, Suh DH, Kim JW. Major clinical research advances in gynecologic cancer in 2020. *J Gynecol Oncol* 2021;32:e53.
[PUBMED](#) | [CROSSREF](#)
3. Ozols RF. Treatment goals in ovarian cancer. *Int J Gynecol Cancer* 2005;15 Suppl 1:3-11.
[PUBMED](#) | [CROSSREF](#)
4. Yancik R. Ovarian cancer. Age contrasts in incidence, histology, disease stage at diagnosis, and mortality. *Cancer* 1993;71 Suppl:517-23.
[PUBMED](#) | [CROSSREF](#)
5. Mrkvová Z, Uldrijan S, Pombinho A, Bartůněk P, Slaninová I. Benzimidazoles downregulate Mdm2 and MdmX and activate p53 in MdmX overexpressing tumor cells. *Molecules* 2019;24:2152.
[PUBMED](#) | [CROSSREF](#)
6. Duan Q, Liu Y, Rockwell S. Fenbendazole as a potential anticancer drug. *Anticancer Res* 2013;33:355-62.
[PUBMED](#)
7. Dogra N, Kumar A, Mukhopadhyay T. Fenbendazole acts as a moderate microtubule destabilizing agent and causes cancer cell death by modulating multiple cellular pathways. *Sci Rep* 2018;8:11926.
[PUBMED](#) | [CROSSREF](#)
8. Tang Y, Liang J, Wu A, Chen Y, Zhao P, Lin T, et al. Co-delivery of trichosanthin and albendazole by nano-self-assembly for overcoming tumor multidrug-resistance and metastasis. *ACS Appl Mater Interfaces* 2017;9:26648-64.
[PUBMED](#) | [CROSSREF](#)
9. Chu SW, Badar S, Morris DL, Pourgholami MH. Potent inhibition of tubulin polymerisation and proliferation of paclitaxel-resistant 1A9PTX22 human ovarian cancer cells by albendazole. *Anticancer Res* 2009;29:3791-6.
[PUBMED](#)
10. Son DS, Lee ES, Adunyah SE. The antitumor potentials of benzimidazole anthelmintics as repurposing drugs. *Immune Netw* 2020;20:e29.
[PUBMED](#) | [CROSSREF](#)
11. Pourgholami MH, Yan Cai Z, Lu Y, Wang L, Morris DL. Albendazole: a potent inhibitor of vascular endothelial growth factor and malignant ascites formation in OVCAR-3 tumor-bearing nude mice. *Clin Cancer Res* 2006;12:1928-35.
[PUBMED](#) | [CROSSREF](#)

12. Choi EK, Kim SW, Nam EJ, Paek J, Yim GW, Kang MH, et al. Differential effect of intraperitoneal albendazole and paclitaxel on ascites formation and expression of vascular endothelial growth factor in ovarian cancer cell-bearing athymic nude mice. *Reprod Sci* 2011;18:763-71.
[PUBMED](#) | [CROSSREF](#)
13. Pourgholami MH, Cai ZY, Chu SW, Galettis P, Morris DL. The influence of ovarian cancer induced peritoneal carcinomatosis on the pharmacokinetics of albendazole in nude mice. *Anticancer Res* 2010;30:423-8.
[PUBMED](#)
14. Dayan AD. Albendazole, mebendazole and praziquantel. Review of non-clinical toxicity and pharmacokinetics. *Acta Trop* 2003;86:141-59.
[PUBMED](#) | [CROSSREF](#)
15. Ye H, Karim AA, Loh XJ. Current treatment options and drug delivery systems as potential therapeutic agents for ovarian cancer: a review. *Mater Sci Eng C Mater Biol Appl* 2014;45:609-19.
[PUBMED](#) | [CROSSREF](#)
16. Kapoor DN, Bhatia A, Kaur R, Sharma R, Kaur G, Dhawan S. PLGA: a unique polymer for drug delivery. *Ther Deliv* 2015;6:41-58.
[PUBMED](#) | [CROSSREF](#)
17. Hickey T, Kreutzer D, Burgess DJ, Moussy F. Dexamethasone/PLGA microspheres for continuous delivery of an anti-inflammatory drug for implantable medical devices. *Biomaterials* 2002;23:1649-56.
[PUBMED](#) | [CROSSREF](#)
18. Byeon Y, Lee JW, Choi WS, Won JE, Kim GH, Kim MG, et al. CD44-targeting PLGA nanoparticles incorporating paclitaxel and FAK siRNA overcome chemoresistance in epithelial ovarian cancer. *Cancer Res* 2018;78:6247-56.
[PUBMED](#) | [CROSSREF](#)
19. Saad AS, Attia AK, Alaraki MS, Elzanfaly ES. Comparative study on the selectivity of various spectrophotometric techniques for the determination of binary mixture of fenbendazole and rafoxanide. *Spectrochim Acta A Mol Biomol Spectrosc* 2015;150:682-90.
[PUBMED](#) | [CROSSREF](#)
20. Heo EJ, Cho YJ, Cho WC, Hong JE, Jeon HK, Oh DY, et al. Patient-derived xenograft models of epithelial ovarian cancer for preclinical studies. *Cancer Res Treat* 2017;49:915-26.
[PUBMED](#) | [CROSSREF](#)
21. Oh DY, Kim S, Choi YL, Cho YJ, Oh E, Choi JJ, et al. HER2 as a novel therapeutic target for cervical cancer. *Oncotarget* 2015;6:36219-30.
[PUBMED](#) | [CROSSREF](#)
22. de Silva N, Guyatt H, Bundy D. Anthelmintics. A comparative review of their clinical pharmacology. *Drugs* 1997;53:769-88.
[PUBMED](#) | [CROSSREF](#)
23. Park H, Lim W, You S, Song G. Fenbendazole induces apoptosis of porcine uterine luminal epithelial and trophoblast cells during early pregnancy. *Sci Total Environ* 2019;681:28-38.
[PUBMED](#) | [CROSSREF](#)
24. Peng Y, Pan J, Ou F, Wang W, Hu H, Chen L, et al. Fenbendazole and its synthetic analog interfere with HeLa cells' proliferation and energy metabolism via inducing oxidative stress and modulating MEK3/6-p38-MAPK pathway. *Chem Biol Interact* 2022;361:109983.
[PUBMED](#) | [CROSSREF](#)
25. Michaelis M, Agha B, Rothweiler F, Löschmann N, Voges Y, Mittelbronn M, et al. Identification of flubendazole as potential anti-neuroblastoma compound in a large cell line screen. *Sci Rep* 2015;5:8202.
[PUBMED](#) | [CROSSREF](#)
26. Sasaki J, Ramesh R, Chada S, Gomyo Y, Roth JA, Mukhopadhyay T. The anthelmintic drug mebendazole induces mitotic arrest and apoptosis by depolymerizing tubulin in non-small cell lung cancer cells. *Mol Cancer Ther* 2002;1:1201-9.
[PUBMED](#)
27. Mukhopadhyay T, Sasaki J, Ramesh R, Roth JA. Mebendazole elicits a potent antitumor effect on human cancer cell lines both in vitro and in vivo. *Clin Cancer Res* 2002;8:2963-9.
[PUBMED](#)
28. Lin S, Yang L, Yao Y, Xu L, Xiang Y, Zhao H, et al. Flubendazole demonstrates valid antitumor effects by inhibiting STAT3 and activating autophagy. *J Exp Clin Cancer Res* 2019;38:293.
[PUBMED](#) | [CROSSREF](#)
29. Nitulescu GM, Van De Venter M, Nitulescu G, Ungurianu A, Juzenas P, Peng Q, et al. The Akt pathway in oncology therapy and beyond (review). *Int J Oncol* 2018;53:2319-31.
[PUBMED](#) | [CROSSREF](#)

30. Pourgholami MH, Wangoo KT, Morris DL. Albendazole-cyclodextrin complex: enhanced cytotoxicity in ovarian cancer cells. *Anticancer Res* 2008;28:2775-9.
[PUBMED](#)
31. Pillai K, Akhter J, Morris DL. Super aqueous solubility of albendazole in β -cyclodextrin for parenteral application in cancer therapy. *J Cancer* 2017;8:913-23.
[PUBMED](#) | [CROSSREF](#)
32. Noorani L, Stenzel M, Liang R, Pourgholami MH, Morris DL. Albumin nanoparticles increase the anticancer efficacy of albendazole in ovarian cancer xenograft model. *J Nanobiotechnology* 2015;13:25.
[PUBMED](#) | [CROSSREF](#)
33. Marslin G, Siram K, Liu X, Khandelwal VK, Xiaolei S, Xiang W, et al. Solid lipid nanoparticles of albendazole for enhancing cellular uptake and cytotoxicity against U-87 MG glioma cell lines. *Molecules* 2017;22:2040.
[PUBMED](#) | [CROSSREF](#)
34. Esfahani MK, Alavi SE, Cabot PJ, Islam N, Izake EL. Pegylated mesoporous silica nanoparticles (MCM-41): a promising carrier for the targeted delivery of fenbendazole into prostate cancer cells. *Pharmaceutics* 2021;13:1605.
[PUBMED](#) | [CROSSREF](#)
35. Kirtane AR, Kalscheuer SM, Panyam J. Exploiting nanotechnology to overcome tumor drug resistance: challenges and opportunities. *Adv Drug Deliv Rev* 2013;65:1731-47.
[PUBMED](#) | [CROSSREF](#)
36. Acharya S, Sahoo SK. PLGA nanoparticles containing various anticancer agents and tumour delivery by EPR effect. *Adv Drug Deliv Rev* 2011;63:170-83.
[PUBMED](#) | [CROSSREF](#)
37. Zhu X, Yan S, Xiao F, Xue M. PLGA nanoparticles delivering CPT-11 combined with focused ultrasound inhibit platinum resistant ovarian cancer. *Transl Cancer Res* 2021;10:1732-43.
[PUBMED](#) | [CROSSREF](#)
38. Domínguez-Ríos R, Sánchez-Ramírez DR, Ruiz-Saray K, Ocegüera-Basurto PE, Almada M, Juárez J, et al. Cisplatin-loaded PLGA nanoparticles for HER2 targeted ovarian cancer therapy. *Colloids Surf B Biointerfaces* 2019;178:199-207.
[PUBMED](#) | [CROSSREF](#)
39. Wang Y, Qiao X, Yang X, Yuan M, Xian S, Zhang L, et al. The role of a drug-loaded poly (lactic co-glycolic acid) (PLGA) copolymer stent in the treatment of ovarian cancer. *Cancer Biol Med* 2020;17:237-50.
[PUBMED](#) | [CROSSREF](#)